Available online at www.sciencedirect.com

ScienceDirect

Biochimica et Biophysica Acta 1768 (2007) 688–693

Biochimica et Biophysica Acta BBA

www.elsevier.com/locate/bbamem

Aquaporin-11 containing a divergent NPA motif has normal water channel activity

Kaya Yakata [a], Yoko Hiroaki [a,b], Kenichi Ishibashi [c], Eisei Sohara [d], Sei Sasaki [d], Kaoru Mitsuoka [e,*], Yoshinori Fujiyoshi [a,b,e]

[a] *Department of Biophysics, Faculty of Science, Kyoto University, Oiwake, Kitashirakawa, Sakyo-ku Kyoto 606-8502, Japan*

[b] *Core Research for Evolution Science and Technology (CREST), Japan Science and Technology Agency (JST), Oiwake, Kitashirakawa, Sakyo-ku, Kyoto 606-8502, Japan*

[c] *Clinical Research Center, Chiba-East National Hospital, Chiba 260-8712, Japan*

[d] *Department of Nephrology, Graduate School of Medicine, Tokyo Medical and Dental University, 1-5-45, Yushima, Bunkyo-ku, Tokyo 113-8519, Japan*

[e] *Japan Biological Information Research Center (JBIRC), The National Institute of Advanced Industrial Science and Technology (AIST), 2-41-6 Aomi, Koto-ku, Tokyo 135-0064, Japan*

Received 8 September 2006; received in revised form 31 October 2006; accepted 8 November 2006
Available online 11 November 2006

Abstract

Recently, two novel mammalian aquaporins (AQPs), AQPs 11 and 12, have been identified and classified as members of a new AQP subfamily, the "subcellular AQPs". In members of this subfamily one of the two asparagine–proline–alanine (NPA) motifs, which play a crucial role in selective water conduction, are not completely conserved. Mouse AQP11 (mAQP11) was expressed in Sf9 cells and purified using the detergent Fos-choline 10. The protein was reconstituted into liposomes, which were used for water conduction studies with a stopped-flow device. Single water permeability (*pf*) of AQP11 was measured to be $1.72 \pm 0.03 \times 10^{-13}$ cm^3/s, suggesting that other members of the subfamily with incompletely conserved NPA motifs may also function as water channels.

Keywords: Subcellular-aquaporin; Asparagine–proline–alanine (NPA)-motif; Baculovirus; Fos-choline 10; Stopped-flow

1. Introduction

The aquaporin (AQP) family of transmembrane channels is divided into two subgroups: water-specific channels (aquaporins) and channels that also permeate small, uncharged solutes such as glycerol (aquaglyceroporins) [1,2]. All AQPs have homologous amino acid sequences consisting of two homologous halves, each containing a highly conserved asparagine–proline–alanine (NPA) motif. All AQPs also share the same unique three-dimensional (3D) fold named the aquaporin fold [3]. In humans, eleven AQPs (AQP0–AQP10) have been identified and functionally characterized [1,2,4]. Three mammalian aquaporins, AQP0, AQP1 and AQP4, have also been structurally analyzed [3,5–9]. The structures revealed that the two NPA motifs play an important role in water permeation through AQPs and especially in proton exclusion, which was explained by the H-bond isolation mechanism [3]. It was therefore thought that changes in the NPA motifs would compromise the proper functioning of AQP water channels.

Recently two new AQPs have been reported in mammals, which were named AQP11 and AQP12 [4,10,11]. Northern blot analysis of rat tissues localized AQP11 to testis, kidney, liver and brain, while AQP12 appears to be specifically expressed in the pancreas. The most remarkable feature of the two new AQPs is their unusual sequence of the first NPA motif: NPC in AQP11 and NPT in AQP12 (Fig. 1). The GenBank database contains several other members of the AQP family with such incompletely conserved NPA motifs, which were recently proposed to form a new AQP subfamily, the "subcellular AQPs" [12].

Abbreviations: AQP, aquaporin; NPA motif, asparagine–proline–alanine motif; ER, endoplasmic reticulum; SIPs, small basic intrinsic proteins; DMPC, dimyristoylphosphatidylcholine; SuD, single channel density

* Corresponding author. Tel.: +81 3 3599 8264; fax: +81 3 3599 8099.
E-mail address: kaorum@jbirc.aist.go.jp (K. Mitsuoka).

0005-2736/$ - see front matter © 2006 Elsevier B.V. All rights reserved.
doi:10.1016/j.bbamem.2006.11.005

```
mAQP1   67  -VGHISGAHLNPAVTLGLLLS-  86
mAQP4   88  -FGHISGGHINPAVTVAMVCT-  107
mAQP8   83  -LGNISGGHFNPAVSLAVTVI-  102
mAQP11  90  -GLTLVGTASNPCGVMMQMIL-  109
mAQP12  84  -GVTFDGASANPTVALQEFLM-  103

mAQP1   183  -AIDYTGCGINPARSFGSAVLTR-  204
mAQP4   204  -AINYTGASMNPARSFGPAVIMG-  225
mAQP8   201  -GGSISGACMNPARAFGPAVMAG-  222
mAQP11  207  -GGSLTGALFNPALALSLHFPCF-  228
mAQP12  203  -GGSLTGAFFNPALAASVTFHCP-  224
```

Fig. 1. Mouse AQP sequences around the two NPA motifs. The boxes indicate the positions of the NPA motifs. While the second NPA motifs in mouse AQPs 11 and 12 are normal, the first NPA motifs are unusual, as the alanine in the motifs are substituted by a cystein residue in AQP11 and a threonine residue in AQP12.

AQP11 knock-out mice are born normal but die before weaning due to uremia from polycystic kidneys [4,10]. Their proximal tubular cells are unusually swollen and contain multiple giant vacuoles. Ribosomes are attached to some of the vacuoles, suggesting that they originate from the endoplasmic reticulum (ER). Furthermore, immunofluorescence microscopy showed that AQP11 is indeed localized to the ER [10]. These findings indicate that AQP11, like AQP6 and AQP8 [13,14], is an intracellular AQP, and that its biological function is related to the ER.

While contradicted by recent experimental results [15], it had originally been reported that AQP11 expressed in *Xenopus* oocytes is not targeted to the plasma membrane [10]. *Xenopus* oocytes were thus not suitable to characterize the function of AQP11 in a quantitative way, which prompted us to establish an in vitro reconstitution system for this purpose [16]. Here we report the expression and purification of recombinant mouse AQP11 (mAQP11) as well as its functional reconstitution into proteoliposomes and its water permeability characteristics.

2. Materials and methods

2.1. Vector subcloning and baculovirus production

The cDNA for mAQP11 was subcloned into the pBlueBacHis2C vector (Invitrogen). Correct insertion was confirmed by DNA sequencing and restriction enzyme digestion. Baculoviruses containing the mAQP11 cDNA were prepared with the BaculoGold transfection kit (BD Bioscience). Viruses were purified from plaques and amplified in cultured Sf9 cells in spinner flasks. mAQP11 expression was verified by Western blot analysis.

2.2. Expression and purification of mAQP11

Expression of mAQP11 and membrane preparation from Sf9 cells were performed as described before for AQP4 [9]. All further purification steps were carried out at 4 °C. To obtain highly purified mAQP11, a number of membrane stripping reagents and detergents were tested [17]. Membrane stripping was assayed by gently mixing 1 ml of membrane suspension (at a protein concentration of 19.2 mg/ml) with an equal volume of stripping solution (2 M urea, 20 mM CAPS (pH 10.0), 0.2 M NaOH, 1 M NaCl, 2 M NaSCN or 0.2 M Na_2CO_3) [17] and subsequent centrifugation for 45 min at 100,000×*g* in a TLA-100.3 rotor (Beckman). Detergents were tested by incubating 50 µl of membrane suspension for 1 h with 50 µl of detergent solution and subsequent centrifugation for 30 min at 100,000×*g* in a TLA-55 rotor (Beckman). Detergents were purchased from Dojindo, Sigma, Wako and Anatrace. Supernatants and pellets from the membrane stripping and solubilization experiments were analyzed by immunoblotting and silver staining. Results obtained with some representative detergents are shown in Fig. 2B.

Purification of mAQP11 was carried out following the protocol previously established for AQP4 [9] with some minor modifications: membranes from 1 l of cell culture were stripped with 1 M urea in 5 mM Tris (pH 7.5), 1 mM EDTA and centrifuged for 45 min at 100,000×*g* in a JA-30.5 rotor (Beckman). The pellet was homogenized in 5 mM Tris (pH 7.5) by 5 strokes in a Potter-Elvehjem tube (at 1400 rpm) and incubated with 1% (w/v) Fos-choline 10 (Anatrace) in 2.5 mM Tris (pH 7.5), 5 mM $MgCl_2$ for 1 h while rotating. After removing unsolubilized material by centrifugation for 45 min at 100,000×*g* in a JA-30.5 rotor (Beckman), mAQP11 in the supernatant was adsorbed to Ni-NTA resin (QIAGEN) for 3 h. The resin was washed with 15 ml of washing buffer (20 mM L-histidine, 20 mM Tris (pH 7.5), 300 mM NaCl, 1% Fos-choline 10), and mAQP11 was eluted by a 30-min incubation in 500 µl elution buffer (100 mM L-histidine, 20 mM Tris (pH 7.5), 300 mM NaCl, 1% Fos-choline 10). Protein concentrations were assayed by ultraviolet absorption spectrometry and/or the DC protein assay kit (BioRad). Immunoblotting was carried out using rabbit anti-mAQP11 antibodies raised against 15 amino acids at the C-terminus of mAQP11 (CLPWLHNNQMTNKKE) as the primary antibody (kindly provided by Drs. Takata and Matsuzaki).

2.3. Protein reconstitution

Purified mAQP11 was reconstituted into liposomes as described before [18]. Briefly, 12.5 µg or 25 µg of purified protein were gently mixed with 5 mg of dimyristoylphosphatidylcholine (DMPC, Sigma) in 1% Fos-choline 10 and incubated for 20 min at 27 °C. The mixture was rapidly injected into detergent-free buffer (50 mM Tris (pH 7.5), 0.5 mM PMSF) at 27 °C, and centrifuged for 1 h at 120,000×*g*, 4 °C. The pellet was re-suspended in the same buffer at 30 °C and centrifuged for 2 cycles to remove residual detergent. The final pellet was resuspended in 1 ml buffer, filtered through a 0.4 µm filter, and diluted in 50 mM Tris (pH 7.5) to obtain a lipid concentration of approximately 0.2 mg/ml.

2.4. Sucrose gradient centrifugation

Sucrose gradient fractionation was performed as described previously [19] with some minor modifications to confirm that mAQP11 was properly incorporated into the membrane. The sucrose gradient consisted of steps of 0, 5, 15, 20, 25% (w/v) sucrose (400 µl/step) in 20 mM Tris (7.5) and 100 mM NaCl. 200 µl of the liposome suspension was mixed with an equal amount of 60% sucrose in the same buffer, and layered under the preformed sucrose gradient. Centrifugation was carried out at 4 °C for 1 h at 41,000 rpm in a TLS-55 swing rotor (Beckman). Fractions at the six interfaces (about 200 µl each) were collected for analysis by electrophoresis and electron microscopy.

2.5. Stopped-flow analysis

Water permeability of mAQP11 was measured according to the method described by Werten et al. [20]. hAQP1 purified in Fos-choline 10 served as positive control and liposomes without protein as negative control. Liposomes were subjected to an inwardly directed sucrose gradient of 100 mOsm/l by rapid mixing in an SX.18MV stopped-flow spectrometer (Applied Photophysics) at room temperature. Time courses of shrinkage of vesicles were monitored by measuring the intensity of 90° scattered light at a wavelength of 450 nm for 10*s*. The averaged time course, $I(t)$, of the first 1*s* segments was used to fit a single exponential function:

$$I(t) = P1 \cdot \exp(-P2 \cdot t) + P3, \quad (1)$$

The osmotic water permeability coefficient *Pf* and the single channel water permeability *pf* were calculated from the rate constant *k* (=*P2*) as described previously [20]. The average diameters of the liposomes were measured from

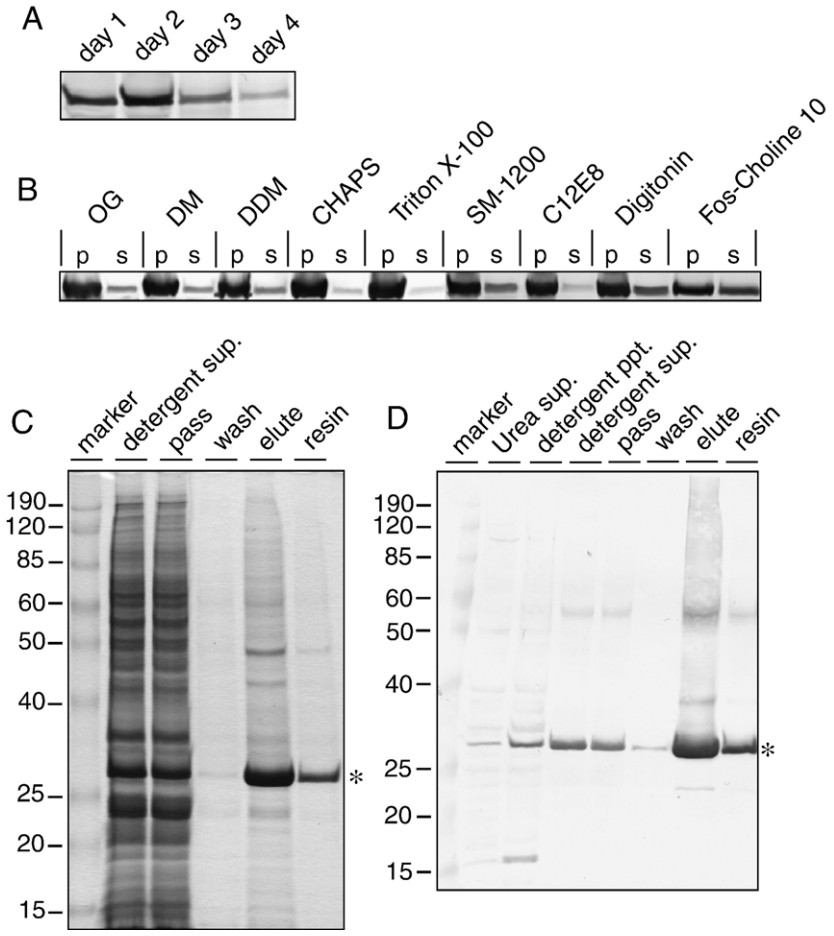

Fig. 2. Expression and purification of mAQP11. (A) Western blot of Sf9 insect cells transfected with mAQP11. 1 ml of cell culture was analyzed 1, 2, 3, and 4 days after infection. Expression of mAQP11 is highest on the second day after infection. (B) Western blot analysis of the solubilization of insect cell membranes with different detergents. OG: octyl-β-D-glucoside, 1.5%; DM: decyl-β-D-maltoside, 1%; DDM: dodecyl-β-D-maltoside, 1%; CHAPS: 3-(dimethylammonio) propanesulfonic acid, 1.5%; Triton X-100: t-octylphenoxypolyethoxyethanol, 1%; SM-1200: sucrose monolaurate, 1%; $C_{12}E_8$: octaethyleneglycol mono-n-dodecyl ether, 1%; Fos-choline 10: N-decylphosphocholine, 1%. "p" and "s" denote pellet and supernatant, respectively. SDS-PAGE analysis of the purification of mAQP11 developed by Coomassie blue staining (C) and immunoblotting (D). The position of the mAQP11 band on the gels is indicated by an asterisk.

electron micrographs of negatively stained samples (examples are shown in Fig. 3A, B). The single channel density (SuD, molecules/cm^2) was calculated as:

$$\mathrm{SuD} = \frac{\mathrm{LSD}}{\mathrm{MW}\cdot \mathrm{LPR}} \cdot 10^{14}, \quad (2)$$

where LSD is the lipid surface density for DMPC of 2.24 kDa/nm^2 [21], MW is the molecular weight of the protein of interest, and LPR is the lipid-to-protein ratio of the proteoliposomes. To calculate the LPR, protein concentrations were estimated from the density of the bands on silver stained SDS-PAGE gels using the program "ImageJ" available on the web (http://rsb.info.nih.gov/ij/). Purified mAQP11 and hAQP1, whose concentrations were determined by DC protein assay, were used to generate standard curves. Lipid concentrations were estimated using the method of Fiske-Subbarow [22].

3. Results

3.1. Expression and purification of mAQP11

His-tagged mAQP11 was expressed in Sf9 insect cells [23] following the protocol we previously established for expression of rat AQP4 [9]. Immunoblot assays showed that the highest

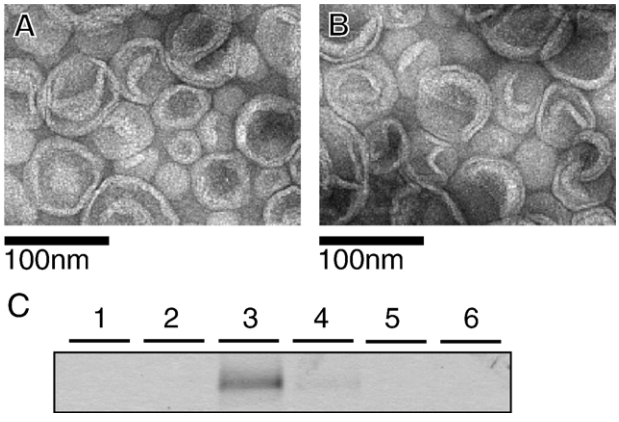

Fig. 3. Protein reconstituted into liposomes. Electron micrographs of proteoliposomes containing mAQP11 (A) or hAQP1 (B) were used to measure the approximate size of the vesicles. (C) Sucrose gradient analysis of reconstituted proteoliposomes. The silver stained gel shows that only fraction 3 contains a band with a molecular weight consistent with that of mAQP11. Negative stain electron microscopy was used to verify that fraction 3 contained liposomes (data not shown).

expression level was reached on the second day after infection (Fig. 2A). Reagents were screened to strip non-integral proteins from isolated membranes, and 1 M urea appeared to be most effective for this purpose. Urea stripped membranes were then incubated with a series of detergents, and immunoblotting was used to identify the optimal solubilization conditions (Fig. 2B). Among the detergents tested, Fos-choline 10 was found to be best suited for the efficient solubilization of mAQP11. SDS-PAGE gels developed by Coomassie blue staining (Fig. 2C) and immunoblotting (Fig. 2D) document the purification procedure and demonstrate the high purity of the final mAQP11 preparation. As reported earlier, immunoblotting showed that the size of His-tagged mAQP11 was about 30 kDa, which was smaller than calculated size of 36 kDa [10]. A key point for obtaining highly concentrated mAQP11 was to add 5 mM $MgCl_2$ to the solubilization buffer. The magnesium ions remarkably improved the efficiency with which His-tagged mAQP11 adsorbed to Ni-NTA resin, while having no apparent effect on the solubilization from the isolated membranes. With the described protocol, we routinely obtained ~1.3 mg of mAQP11 from 1 l of Sf9 cell culture.

3.2. Functional analysis of reconstituted protein

To assess the biological function of the recombinant protein, purified mAQP11 was reconstituted into vesicles using the rapid dilution method [18]. The proteoliposomes were then subjected to an inwardly directed osmotic gradient and their shrinkage over time was measured by monitoring the intensity of scattered light in a stopped-flow device (Fig. 4) [20]. The shape and size of the proteoliposomes were determined by negative stain electron microscopy (typical images are shown in Fig. 3A, B). The proper integration of mAQP11 into the liposomes was verified by sucrose gradient fractionation (Fig. 3C) [19]. Liposomes containing human AQP1 (hAQP1) were used as positive controls and liposomes without reconstituted protein as negative controls. Table 1 shows the averaged *pf* values for mAQP11 and hAQP1. Despite the incompletely conserved NPA motif, mAQP11 showed very high water permeability, $1.72 \pm 0.03 \times 10^{-13}$ cm^3/s, comparable in magnitude to that of AQP1, 1.17×10^{-13} cm^3/s [18].

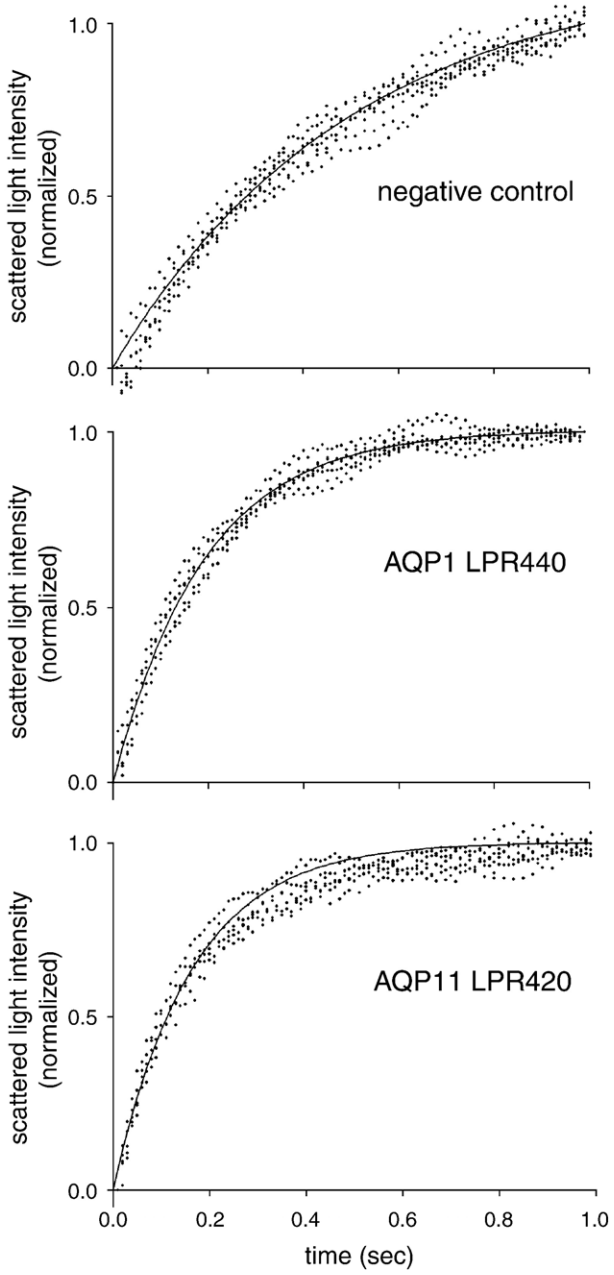

Fig. 4. Stopped-flow analysis of mAQP11 and hAQP1 reconstituted into lipid vesicles. Proteoliposomes (or liposomes as negative control) were rapidly subjected to an inwardly directed osmotic gradient of sucrose while monitoring the shrinkage of the vesicles. The LPR of the proteoliposomes was obtained as described in Materials and methods. The dots are values for individual experiments (to avoid excessive overlap only five data points are shown that were randomly selected from all measured data) for pure DMPC liposomes ($n=28$, top), hAQP1 proteoliposomes (LPR 440, $n=51$, middle) and mAQP11 proteoliposomes (LPR 420, $n=48$, bottom). The curves show single exponential functions fit to the averaged time courses.

4. Discussion

We succeeded in the heterologous expression, purification and functional characterization of mAQP11. Despite the intracellular localization in the proximal tubule, AQP11 has been reported to reach the plasma membrane in *Xenopus* oocytes and to have poor water permeability [15]. However, to characterize the function of AQP11 in a more quantitative way, a more detailed analysis was required [16]. In the process of establishing a purification protocol for mAQP11, we found that Fos-cholines were the only detergents with which mAQP11 could be efficiently solubilized from insect cell membranes without causing the protein to denature and precipitate. Even octyl glucoside, a detergent that has successfully been used for the solubilization of several other AQPs, failed to keep mAQP11 stably in solution. This may be attributed to the localization of AQP11 to intracellular membranes, which may require the use of detergents with different physicochemical characteristics than those typically used for the solubilization of integral proteins from the plasma membrane. Another interesting finding we made in the purification of mAQP11 was that a small concentration of Mg^{2+} in the solubilization buffer

Table 1
Water flow through reconstituted hAQP1 and mAQP11

	mAQP11		Positive control (hAQP1)		Negative control
	LPR 210 (n=43)	LPR 420 (n=48)	LPR 320 (n=43)	LPR 440 (n=51)	(n=28)
d (cm)	7.0×10^{-6}	7.0×10^{-6}	7.0×10^{-6}	7.0×10^{-6}	4.0×10^{-6}
k (s^{-1})	9.53±0.15	6.18±0.13	7.16±0.16	5.26±0.05	2.00±0.05
Pf (cm/s)	$6.18\pm0.10\times10^{-3}$	$4.00\pm0.08\times10^{-3}$	$4.64\pm0.10\times10^{-3}$	$3.41\pm0.03\times10^{-3}$	$7.41\pm0.20\times10^{-4}$
SuD (cm^{-2})	3.50×10^{10}	1.75×10^{10}	2.43×10^{10}	1.77×10^{10}	–
pf (cm^3/s)	$1.56\pm0.03\times10^{-13}$	$1.87\pm0.05\times10^{-13}$	$1.61\pm0.04\times10^{-13}$	$1.51\pm0.02\times10^{-13}$	–
pf (H_2O/s)	$5.22\pm0.10\times10^{9}$	$6.25\pm0.17\times10^{9}$	$5.38\pm0.13\times10^{9}$	$5.05\pm0.07\times10^{9}$	–

The pf values of the proteoliposomes were calculated by subtracting the Pf of the negative control from each Pf value and then dividing the number by the corresponding SuD value. d, k, Pf and SuD were calculated as described in Materials and methods. The last line denotes the number of water molecules that permeate a single subunit per second.

remarkably improved the capacity of His-tagged mAQP11 to bind to Ni-NTA resin. It may be that addition of Mg^{2+} reduces the thickness of the surrounding detergent layer, possibly by an interaction of the positively charged magnesium ions with the phosphate group of Fos-choline 10.

Our results show that the alanine-to-cysteine substitution in the first NPA motif does not negatively affect the water permeability of mAQP11. Some plants also express AQPs whose alanine in the first NPA motifs are substituted by other residues and are localized in the ER. Some of these AQPs, named SIPs for *s*mall basic *i*ntrinsic *p*roteins, have been shown to permeate water [24,25]. The importance of the Asn residues in the two NPAs is however undisputed from physiological [26] and structural studies [3,5,27].

Here we demonstrate that AQP11, known to be localized in the ER, functions as an efficient water channel. The pf value measured for recombinant mAQP11 is similar in magnitude to that of hAQP1, which we used as positive control and whose pf value has previously been determined [18,28]. Quantitative analysis of hAQP1 water permeability with the His-tag sequence showed the pf (H_2O/s) of $5.05\pm0.07\times10^9$, which is the same with that of hAQP1 without His-tag sequence [18,28]. Therefore the presence of a His-tag had no influence on the water conduction characteristics of reconstituted AQP1. Based on quantitative analysis of AQP1, we did not remove the His-tag from mAQP11 for our activity measurements. It has been reported that ER membranes of renal proximal tubular cells display water permeability that is sensitive to $HgCl_2$ [29], but AQP11 does not have a cysteine residue at the critical position that makes other AQPs mercury sensitive, e.g. Cys189 in AQP1 [3]. Therefore, some other AQPs may be expressed in the ER membrane that is sensitive to mercury. It was also reported that AQP11 knock-out mice display a delay in endosomal acidification while no defect was observed in the concentration of chloride ions [10]. AQP8, which has the highest homology to AQP11 among the conventional aquaporins (AQP0–AQP10) [4], was implicated in mediating osmotic water movement across the membrane of glycogen-storing vesicles in hepatocytes [30]. It is thus attractive to speculate that AQP11 may buffer changes in osmotic pressure caused by the accumulation of solutes such as inorganic ions, organic ions, translated proteins and/or protons in the ER and endosomes, and therefore may help to maintain homeostasis of these organelles. Further functional as well as structural studies on AQP11 will be needed to characterize all its functions and to fully understand its physiological roles. The expression and purification procedures for mAQP11 reported here should greatly aid these future investigations.

Acknowledgements

We acknowledge Dr. Kuniaki Takata and Dr. Toshiyuki Matsuzaki for providing anti-mAQP11 antibody. We acknowledge Dr. Thomas Walz for his critical reading and valuable comments. This research was supported by Grants-in-Aid for Specially Promoted Research, Grant-in-Aid for 21st Century COE Research Kyoto University (A2), the Japan Science and Technology Agency (JST), and the Japan New Energy and Industrial Technology Development Organization (NEDO).

References

[1] L.S. King, D. Kozono, P. Agre, From structure to disease: the evolving tale of aquaporin biology, Nat. Rev., Mol. Cell Biol. 5 (2004) 687–698.
[2] P. Agre, L.S. King, M. Yasui, W.B. Guggino, O.P. Ottersen, Y. Fujiyoshi, A. Engel, S. Nielsen, Topical review: aquaporin water channels—from atomic structure to clinical medicine, J. Physiol. 542 (2002) 3–16.
[3] K. Murata, K. Mitsuoka, T. Hirai, T. Walz, P. Agre, J.B. Heymann, A. Engel, Y. Fujiyoshi, Structural determinants of water permeation through aquaporin-1, Nature 407 (2000) 599–605.
[4] Y. Morishita, Y. Sakube, S. Sasaki, K. Ishibashi, Molecular mechanisms and drug development in aquaporin water channel diseases: aquaporin super family (superaquaporins): expansion of aquaporins restricted to multicellular organisms, J. Pharmacol. Sci. 96 (2004) 276–279.
[5] T. Gonen, Y. Cheng, P. Sliz, Y. Hiroaki, Y. Fujiyoshi, S.C. Harrison, T. Walz, Lipid–protein interactions in double-layered two-dimensional AQP0 crystals, Nature 438 (2005) 633–638.
[6] W.E. Harries, D. Akhavan, L.J. Miercke, S. Khademi, R.M. Stroud, The channel architecture of aquaporin 0 at a 2.2-A resolution, Proc. Natl. Acad. Sci. U. S. A. 101 (2004) 14045–14050.
[7] H. Sui, B.G. Han, J.K. Lee, P. Walian, B.K. Jap, Structural basis of water-specific transport through the AQP1 water channel, Nature 414 (2001) 872–878.
[8] G. Ren, V.S. Reddy, A. Cheng, P. Melnyk, A.K. Mitra, Visualization of a water-selective pore by electron crystallography in vitreous ice, Proc. Natl. Acad. Sci. U. S. A. 98 (2001) 1398–1403.
[9] Y. Hiroaki, K. Tani, A. Kamegawa, N. Gyobu, K. Nishikawa, H. Suzuki, T. Walz, S. Sasaki, K. Mitsuoka, K. Kimura, A. Mizoguchi, Y. Fujiyoshi, Implications of the aquaporin-4 structure on array formation and cell adhesion, J. Mol. Biol. 355 (2006) 628–639.
[10] Y. Morishita, T. Matsuzaki, M. Hara-chikuma, A. Andoo, M. Shimono, A. Matsuki, K. Kobayashi, M. Ikeda, T. Yamamoto, A. Verkman, E. Kusano, S. Ookawara, K. Takata, S. Sasaki, K. Ishibashi, Disruption of aquaporin-

11 produces polycystic kidneys following vacuolization of the proximal tubule, Mol. Cell. Biol. 25 (2005) 7770–7779.
[11] T. Itoh, T. Rai, M. Kuwahara, S.B. Ko, S. Uchida, S. Sasaki, K. Ishibashi, Identification of a novel aquaporin, AQP12, expressed in pancreatic acinar cells, Biochem. Biophys. Res. Commun. 330 (2005) 832–838.
[12] K. Ishibashi, Aquaporin subfamily with unusual NPA boxes, Biochim. Biophys. Acta 1758 (2006) 989–993.
[13] M. Yasui, A. Hazama, T.H. Kwon, S. Nielsen, W.B. Guggino, P. Agre, Rapid gating and anion permeability of an intracellular aquaporin, Nature 402 (1999) 184–187.
[14] M.L. Elkjaer, L.N. Nejsum, V. Gresz, T.H. Kwon, U.B. Jensen, J. Frokiaer, S. Nielsen, Immunolocalization of aquaporin-8 in rat kidney, gastrointestinal tract, testis, and airways, Am. J. Physiol.: Renal Physiol. 281 (2001) 1047–1057.
[15] D.A. Gorelick, J. Praetorius, T. Tsunenari, S. Nielsen, P. Agre, Aquaporin-11: a channel protein lacking apparent transport function expressed in brain, BMC Biochem. 7 (2006) 14.
[16] K. Liu, H. Nagase, C.G. Huang, G. Calamita, P. Agre, Purification and functional characterization of aquaporin-8, Biol. Cell 98 (2006) 153–161.
[17] B. Yang, A.N. van Hoek, A.S. Verkman, Very high single channel water permeability of aquaporin-4 in baculovirus-infected insect cells and liposomes reconstituted with purified aquaporin-4, Biochemistry 36 (1997) 7625–7632.
[18] M.L. Zeidel, S.V. Ambudkar, B.L. Smith, P. Agre, Reconstitution of functional water channels in liposomes containing purified red cell CHIP28 protein, Biochemistry 31 (1992) 7436–7440.
[19] J.L. Rigaud, M.T. Paternostre, A. Bluzat, Mechanisms of membrane protein insertion into liposomes during reconstitution procedures involving the use of detergents. 2. Incorporation of the light-driven proton pump bacteriorhodopsin, Biochemistry 27 (1988) 2677–2688.
[20] P.J. Werten, L. Hasler, J.B. Koenderink, C.H. Klaassen, W.J. de Grip, A. Engel, P.M. Deen, Large-scale purification of functional recombinant human aquaporin-2, FEBS Lett. 504 (2001) 200–205.
[21] N. Kucerka, Y. Liu, N. Chu, H.I. Petrache, S. Tristram-Nagle, J.F. Nagle, Structure of fully hydrated fluid phase DMPC and DLPC lipid bilayers using X-ray scattering from oriented multilamellar arrays and from unilamellar vesicles, Biophys. J. 88 (2005) 2626–2637.
[22] C.H. Fiske, Y. Subbarow, The colorimetric determination of phosphorus, J. Biol. Chem. 66 (1925) 375–400.
[23] M.D. Summers, G.E. Smith, A Manual of Methods for Baculovirus Vectors and Insect Cell Culture Procedures, The Texas Agricultural Experiment Station, The Texas A & M University System College Station, Texas, 1987.
[24] U. Johanson, S. Gustavsson, A new subfamily of major intrinsic proteins in plants, Mol. Biol. Evol. 19 (2002) 456–461.
[25] F. Ishikawa, S. Suga, T. Uemura, M.H. Sato, M. Maeshima, Novel type aquaporin SIPs are mainly localized to the ER membrane and show cell-specific expression in *Arabidopsis thaliana*, FEBS Lett. 579 (2005) 5814–5820.
[26] S. Chretien, J.P. Catron, A single mutation inside the NPA motif of aquaporin-1 found in a Colton-null phenotype, Blood 93 (1999) 4021–4023.
[27] E. Tajkhorshid, P. Nollert, M.O. Jensen, L.J. Miercke, J. O'Connell, R.M. Stroud, K. Schulten, Control of the selectivity of the aquaporin water channel family by global orientational tuning, Science 296 (2002) 525–530.
[28] A.N. van Hoek, A.S. Verkman, Functional reconstitution of the isolated erythrocyte water channel CHIP28, J. Biol. Chem. 267 (1992) 18267–18269.
[29] F.G. van der Goot, R.A. Podevin, B.J. Corman, Water permeabilities and salt reflection coefficients of luminal, basolateral and intracellular membrane vesicles isolated from rabbit kidney proximal tubule, Biochim. Biophys. Acta 986 (1989) 332–340.
[30] D. Ferri, A. Mazzone, G.E. Liquori, G. Cassano, M. Svelto, G. Calamita, Ontogeny, distribution, and possible functional implications of an unusual aquaporin, AQP8, in mouse liver, Hepatology 38 (2003) 947–957.